Research Article

Ab initio study of the adsorption of 3*d* transition metals on Ni(100) surface

Mohammad Obeid[1] · Ihsan Erikat[2] · Bothina Hamad[1,3] · Jamil Khalifeh[1]

Received: 30 October 2019 / Accepted: 28 February 2020 / Published online: 13 March 2020

Abstract
Nickel based catalysis has shown high activity, selectivity and stability more than mono-Ni surface catalysis in energy and environmental applications. First principle calculations based on Density Functional Theory and the Generalized Gradient Approximation are performed to investigate the structural, electronic, and magnetic properties of M/Ni(100); M=Fe, Co, and Cu systems at 0.25, 0.50 and 1.00 monolayer coverage. Ferromagnetic (FM) configuration is found to be more stable than non-magnetic configuration for all studied elements. Adsorption of Fe and Co on Ni(100) surface enhances the FM properties of admetal and substrate at all coverage. Whereas, Cu decreases the FM properties of the topmost Ni(100) surface atom and kept almost non-magnetic. The *d* band center is calculated for the admetal and topmost Ni surface atom at all coverages. The obtained results are explained by Hammer- Nørskov model to predict the change on the reactivity of Ni surface by adding the adsorbed metals. The calculations reveal that there is no clear relationship between the *d* band-center and the magnetic moments of the Ni surface layer.

Keywords Adsorption · Magnetization · Bimetal · 3d · Ni · DFT

1 Introduction

Bimetallic catalysts are promising and economical materials for many important processes such as CO oxidation, fuel cells and the partial oxidation of methanol. Bimetallic catalysts have interesting electronic, optical, magnetic properties as well as many technological applications, e.g., in storage technology, magnetic detection techniques and drug delivery [1–5]. The formation of bimetallic catalysts differs significantly from monometallic catalysts due to the mutual promotion as a result of decreasing the metal-support interactions [6]. Moreover, nickel surfaces can be used as carbon sources since they are active for adsorbing and interacting with the hydrocarbons because they have non-filled *d*-shells. However, Ni-based catalysts have higher activity, selectivity and stability than mono-Ni surface catalysts in energy and environmental applications [7–9]. Industrially, Ni-based surfaces are preferred as catalysts for Fischer–Tropsch reaction due to its lower price and high activity [10]. Adding Fe, Co and Cu to Ni catalysts improve the activity of methane reforming [11]. The growth of Fe ultrathin films on Ni(100) surface is investigated by Luches et al. using primary-beam diffraction modulated electron emission (PDMEE) and low-energy electron diffraction (LEED) from 0 to 25 monolayer (ML) coverages. They reported that Fe layers from 1 to 5 deposits on Ni surface as fcc structure with intermixing between Fe and Ni in the first 3 ML [12]. O'Brien and Tonner studied the magnetic phases of Fe on Ni (100) surface using X-ray magnetic circular dichroism. They reported that Fe is FM at coverages below 5 ML with the magnetic moments like that found for Fe on Cu (100) surface [13]. A number of theoretical studies on the overlayer ferromagnetic substrate are reported [14, 15]. Šljivančanin and Vukajlović [13]

✉ Ihsan Erikat, ihsanas2000@gmail.com | [1]Department of Physics, The University of Jordan, Amman 11942, Jordan. [2]Department of Physics, Isra University, Amman, Jordan. [3]Department of Physics, University of Arkansas, Fayetteville, AR 72701, USA.

calculated theoretically the magnetic moment through the interface region including magnetization profile for Ni(111) surface covered by a monolayer or a bilayer of 3*d* and 4*d* transition metals. They found that coating Ni(111) surface with Cu atoms lowers the minority spin of Ni and causes a considerable reduction in the nickel atomic magnetic moment at the observed interface. However, Cu overlayer atom on Ni substrate has a very small magnetic moment since Cu *d* band center is lower than Ni 3*d* band center which causes a very weak hybridization. Niklasson et al. [15] by using first principles Green's function method found that there is no large deviation of the interface magnetization in the Co/Ni interface compared to bulk Co and Ni. Gonzalez-delaCruz et al. [16] reported that bimetallic Co–Ni catalysts have a better activity and stability than the nickel monometallic system due to the strong synergic effect between Ni and Co sites. Moreover, using an experimental method, Zhang et al. reported that the synergy of Ni-Co bimetallic catalysts provides high activity and has outstanding stability. They explained these modified properties for Ni-Co catalysts due to the synergetic effect and good metal dispersion [17]. Also, Wang et al. investigated the factors that control the interaction of CO_2 with transition metals surfaces by using DFT. They reported that both *d* band center and charges transfer between CO_2 and metal surface control the CO_2 interaction. They concluded that the catalytic properties of the material depend on the electronic states near Fermi energy [18]. In this manuscript the effect of the adsorption of 3*d* transition metals on the structural, electronic and magnetic properties of Ni(100) surface is investigated. Also, the *d* band center is calculated for the admetal atoms as well as the Ni topmost atom surface. Moreover, we aim to make trends about the change in the reactivity of the bimetallic surface compared with Ni(100) clean surface according to Hammer- Nørskov model [19].

2 Computational method

Quantum Espresso (QE) code is used to perform spin polarized calculations with a plane wave basis-set [20]. Generalized gradient approximation proposed by Perdew, Burke and Ernzerhof (GGA-PBE) functional [21] is used as exchange correlation potential. The obtained lattice constant for bulk Ni is 3.55 Å which is 0.90% larger than the experimental value (3.52 Å) [22]. The obtained magnetic moment for bulk Ni is 0.69 μ_B while the experimental value is 0.62 μ_B [23]. Slab method is used to simulate the Ni(100) surface with seven (ten) nickel (vacuum) layers. The Brillouin-zone integrations are performed using (12×12×1) and (6×6×1) Monkhorst–Pack (MP) grid [24] for (1×1) and (2×2) unit cells, respectively. The electronic wavefunctions are expanded in a plane wave basis set with 748.55 eV as a cutoff energy. Ultrasoft pseudopotential is used to describe the ionic cores with scalar-relativistic calculations. A Methfessel Paxton smearing [25] with $\sigma = 0.20$ eV is used to improve the computational performance. The adsorbates are placed on both sides of the slab to confirm symmetry and delete the magnetic dipole effects. All atomic positions of the adsorbates and Ni layers are relaxed except these atoms in the central layer, which are frozen in their bulk positions. At the beginning, magnetic and non-magnetic calculations are done for M/Ni(100)–(1×1); M=(Fe, Co and Cu) systems to investigate the most stable structure and test the feasibility of inserting magnetic calculations. The spin polarization energy of the FM order for the adsorbates M; M=Fe, Co and Cu are calculated by using the equation:

$$\Delta E = -(E_{mag} - E_{non-mag})/N \quad (1)$$

With E_{mag} and $E_{non-mag}$ the energy of magnetic and non-magnetic calculations, respectively, and N is the number of adsorbed atoms.

The Projected density of states (PDOS) is plotted to determine the electronic and magnetic properties and the *d* band center of is calculated as the first moment of the projected d-band density of states on the surface atoms referenced to the Fermi level as:

$$\text{center of d band} = \frac{\int_{-\infty}^{0} \in DOS(\in) d \in}{\int_{-\infty}^{0} DOS(\in) d \in} \quad (2)$$

where $\in = E - E_f$, E_f is the Fermi energy and $DOS(\in)$ is the density of states.

3 Results and discussion

The hollow site is found the most stable site for all studied elements on Ni(100) surface at 0.25, 0.50 and 1.00 ML coverages. The adsorption of Fe, Co and Cu on Ni(100) surface is investigated at the hollow site for FM and NM configuration at coverage 1.00 ML. The results reveal that the relaxed systems become more stable by considering the magnetic calculations, which is consistent with previous studies on similar systems (12,13,15). The FM order (ΔE) for the studied metals on (1×1) Ni (100) surface are 2.23, 1.39 and 0.34 eV, for Fe, Co and Cu, respectively in the order of $\Delta E_{Fe} > \Delta E_{Co} > \Delta E_{Cu}$. This is consistent with the bulk magnetic moment of these elements.

3.1 Fe/Ni (100) system

The structural properties for Fe/Ni (100) system are shown in Table 1. The Fe–Ni bond lengths increase as the coverage increases from 0.25ML to 1.00 ML. At 1.00 ML coverage

Table 1 Structural properties for M/Ni (100); M=Fe, Co and Cu. d_{M-M} is M–M bond, d_{M-Ni} is M–Ni bond, d_{Ni-Ni} is Ni–Ni bon and $\Delta d_{i,j}$ is the interlayer distance between Ni *i* and *j* surface layers

System	d_{M-M} Å	d_{M-Ni} Å	d_{Ni-Ni} Å	$\Delta d_{1,2}$ %	$\Delta d_{2,3}$%	$\Delta d_{3,4}$%
Ni (100)				−4.97	−0.83	−1.38
Fe/Ni (100)						
Θ=0.25	5.18	2.31	2.58	−2.55	−1.64	−1.66
Θ=0.50	3.54	2.33	2.51	0.52	−2.04	−1.76
Θ=1.00	2.51	2.50	2.51	−0.29	−0.29	−0.29
Co/Ni (100)						
Θ=0.25	5.02	2.30	2.57	−2.27	−1.56	−1.70
Θ=0.50	3.54	2.32	2.51	−0.12	−1.77	−1.77
Θ=1.00	2.51	2.45	2.51	0.79	−2.40	−1.82
Cu/Ni (100)						
Θ=0.25	5.02	2.44	2.54	−4.40	−1.13	−1.48
Θ=0.50	3.54	2.45	2.51	−3.66	−0.01	−1.20
Θ=1.00	2.51	2.52	2.51	−2.64	−1.88	−1.29

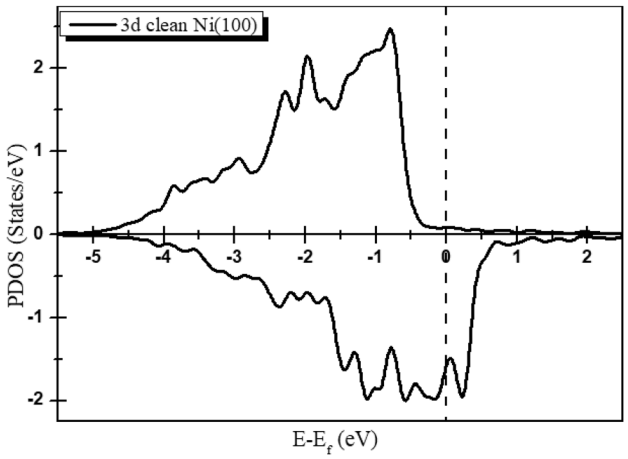

Fig. 1 PDOS of clean Ni(100) surface

Table 2 The *d* band center for M and Ni topmost atom in M/Ni (100) systems in eV

System	Majority- M	Minority- M	Majority Ni (100)	Minority Ni (100)
Clean			−1.93	−1.36
Fe				
Θ=0.25	−3.28	−1.52	−2.08	−1.62
Θ=0.50	−3.43	−1.66	−2.36	−1.93
Θ=1.00	−2.73	−1.31	−2.28	−1.9
Co				
Θ=0.25	−2.85	−1.46	−2.13	−1.63
Θ=0.50	−2.74	−1.31	−2.37	−1.89
Θ=1.00	−2.68	−1.47	−2.37	−1.95
Cu				
Θ=0.25	−2.06	−2.03	−1.94	−1.45
Θ=0.50	−2.01	−1.99	−1.96	−1.53
Θ=1.00	−2.37	−2.37	−1.98	−1.62

the Fe–Fe bond is 2.51 Å same as Ni–Ni bond and equal to the lattice constant of Ni(100) fcc surface. This result indicates the pseudomorphic growth of Fe overlayer on Ni(100) where the admetal usually has a lattice constant that matches the lattice constant of the underlying substance [26]. The interlayer spacing shows an overall contraction except in Δd_{12} for Fe/Ni(100) system at 0.50 ML coverage. The $\Delta d_{1,2}$ interlayer expands in all configurations comparing with its value at clean surface (−4.97%), see Table 1.

The PDOS of the 3*d* band for the topmost Ni surface atom at clean Ni(100) surface is shown in Fig. 1. The majority spin band is nearly full in the Ni surface and almost all this band lies to the left of the Fermi energy. However, the 3*d* minority band spin is partially empty. There are sharp peaks at −0.77, −1.97 and −2.29 eV at the majority spin and −1.47, −0.58, −0.17 and 0.22 eV in the minority spin. The calculated *d* band centres for Ni clean surface are −1.93 and −1.36 eV at the majority and minority spins, respectively, see Table 2. The magnetic moment for the topmost Ni atom at Ni(100) surface increases by about 0.06 μ_B compared to its value at bulk Ni (0.69 μ_B). The PDOS for Fe/Ni(100) system is presented in Fig. 2 at 0.25, 0.50 and 1.00 ML coverage. There is a large energy splitting between the majority and minority spin states *at 3d* Fe which reflects the high magnetic moments of Fe at all coverages. O'Brien and Tonner reported that the magnetic moment of the ultrathin Fe layer enhanced by the adsorption on Ni(100) surface [13]. Also, Šljivančanin and Vukajlović calculated the effect of covering Ni(111) surface by 3*d* and 4*d* transition metals on the magnetic moments of both Ni(111) surface and the covering metals by using

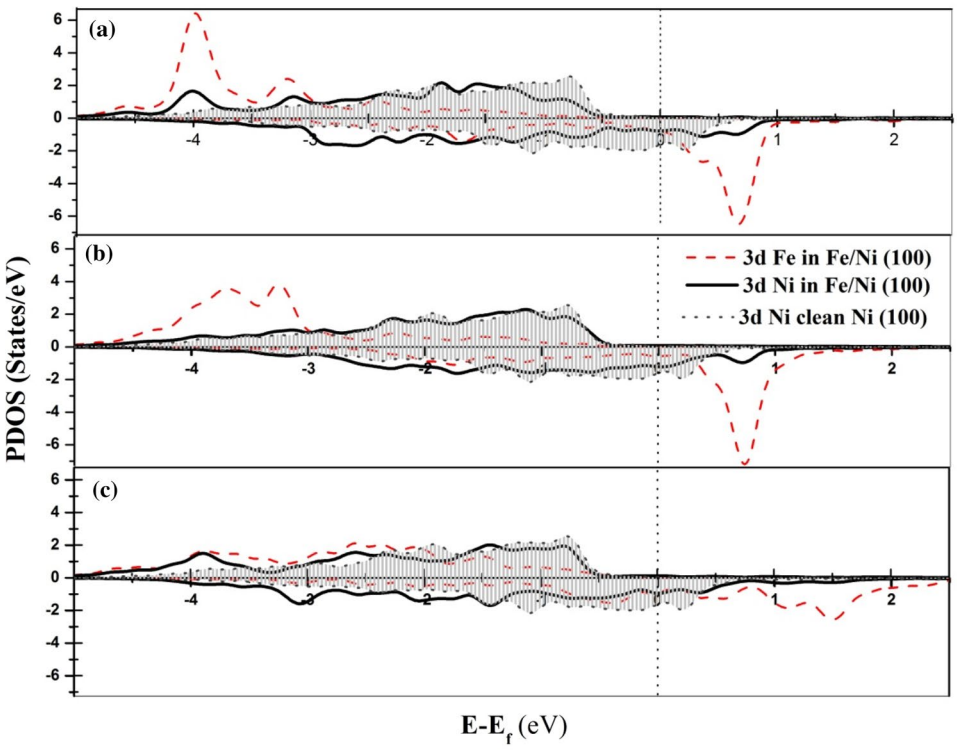

Fig. 2 PDOS of Fe/Ni(100) – (2 × 2) system with different coverages **a** 0.25 ML, **b** 0.50 ML, **c** 1.00 ML. Black solid line for 3*d* Ni topmost atom, red dash line for 3*d* Fe and the dot shaded light grey for 3*d* Ni topmost atom in clean Ni(100) surface. (For interpretation of the references to color in this figure legend, the reader is referred to the web version of the article.)

tight binding linear muffin tin orbitals and Green function technique. They found that covering Ni(111) surface by a monolayer of Fe or Co produces small changes on the magnetic moment of Ni(111) surface. They related these small changes in the magnetic moments of Ni surface to the small exchange splitting between the majority and minority spin bands of Ni fcc metal [14].

There is hybridization between metals overlayer and Ni surface atoms as can be seen from Fig. 2. The 3*d* band hybridization between Fe and Ni is obvious at − 4.05, − 3.15, − 2.37 and 0.55 eV at 0.25 ML coverage.

The *d* band center of the majority (minority) spin for the topmost Ni surface atom at this system shifts to the left compared with *d* band center of the topmost Ni atom at Ni(100) clean surface by 0.15 (0.26), 0.43 (0.57) and 0.35 (0.54) eV, for 0.25, 0.50 and 1.00 ML, respectively. The shift of the *d* band center for Ni surface up in energy from right to left due the *3d* band hybridization between the Ni and Fe predicts the increase in the adsorbate- metal binding energy according to Hammer- Nørskov model [27].

The *d* band center of the majority and minority Fe spin shifts to the left (right) of Fermi energy by 0.15 (0.55) eV and 0.14 (0.21) eV, respectively compared with its value at 0.25 ML coverage as the coverage of Fe increases to 0.50 (1.00) ML, see Table 2. Moreover, the magnetic moment of Fe increases (decreases) by 0.03 (0.33) μ_B as the coverage increases from 0.25 to 0.50 (1.00) ML. The increase in the magnetic moment at 0.50 ML coverage is due to the high Fe–Ni interaction which causes the large expansion of $\Delta d_{1,2}$ at 0.50 ML coverage as can be seen in Table 1 and the largest shift of *d* band to the left compared with other coverages. However, the increase in Fe–Fe interaction at 1.00 ML coverage decreases the *3d* band hybridization between Fe and Ni states and causes a large broadening in the PDOS of Fe.

3.2 Co/Ni(100) system

The structural properties of Co/Ni (100) system are shown in Table 1. The bond lengths increase as the coverage increases from 0.25 ML to 1.00 ML due to the increase in Co–Co interaction. At 1.00 ML coverage Co–Co bond is equal to Ni–Ni bond forming pseudomorphic growth. The Co–Ni bond is smaller than that for Fe–Ni or Cu–Ni at all coverages reflecting the large interaction between Co and Ni surface atoms.

The PDOS for Co/Ni (100) system 0.25, 0.50 and 1.00 ML coverages is shown in Fig. 3. The broadening in Co PDOS increases as the coverage increases. The interaction between 3*d* bands shifts Co high energy empty state to the left as the coverage increases. At 0.50 ML coverage the highest peak of the minority spin in Co PDOS is at Fermi energy. The relative large value of the minority spin PDOS of Co layer at Fermi energy, i.e. compared with Fe/Ni(100) and Cu/Ni (100), see Figs. 2, 3 and 4, refers to the high occupation at Fermi level which indicates the high

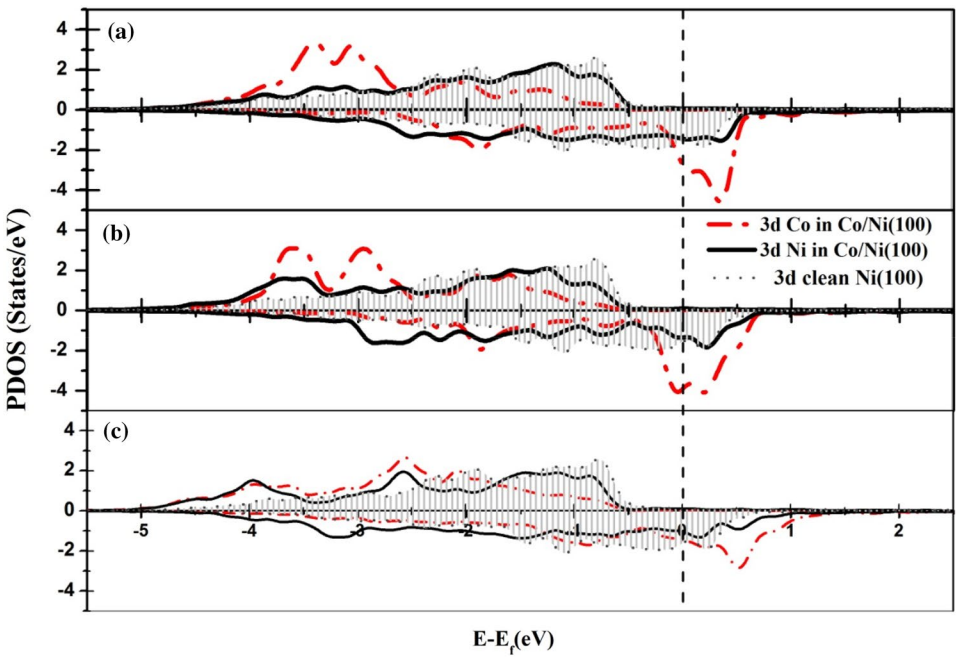

Fig. 3 PDOS of Co/Ni(100) – (2 × 2) system with different coverages **a** 0.25 ML, **b** 0.50 ML, **c** 1.00 ML. Black solid line for 3*d* Ni topmost atom, red dash line for 3*d* Co and dot shaded light grey for 3*d* Ni topmost atom in clean Ni(100) surface (for interpretation of the references to color in this figure legend, the reader is referred to the web version of the article)

activity for this catalyst for the dissociative chemisorption [17, 28]. Also, the magnetic moment of Co decreases as the coverage increase from 0.25 to 0.50 ML as a result of the decrease in the exchange splitting of 3*d* Co states.

The *d* band center of the majority (minority) spin of Ni surface in Co/Ni (100) system shift to the left by 0.20 (0.27), 0.44 (0.53) and 0.44 (0.59) eV for 0.25, 0.50 and 1.00 ML, respectively, relative to its value at Ni(100) clean surface. The *d* band center of the majority (minority) Co spin at 0.50 ML coverage shifts to the right of Fermi energy by 0.11 (0.15) compared with its value at 0.25 ML coverage. Also, the magnetic moments of Ni topmost surface atom in Co/Ni(100) system has the highest value (0.78 μ_B) at 0.50 ML coverage. The *d* band center of the majority (minority) Co spin at 1.00 ML coverage shifts to the right (left) of Fermi energy by 0.17 (0.01) μ_B compared with its value at 0.25 ML coverage. The magnetic moments of Ni topmost surface atom in Co/Ni(100) system decreases to 0.72 μ_B at 1.00 ML coverage. The magnetic moment of Co atoms decreases as the coverage increases as can be seen in Table 3. Moreover,

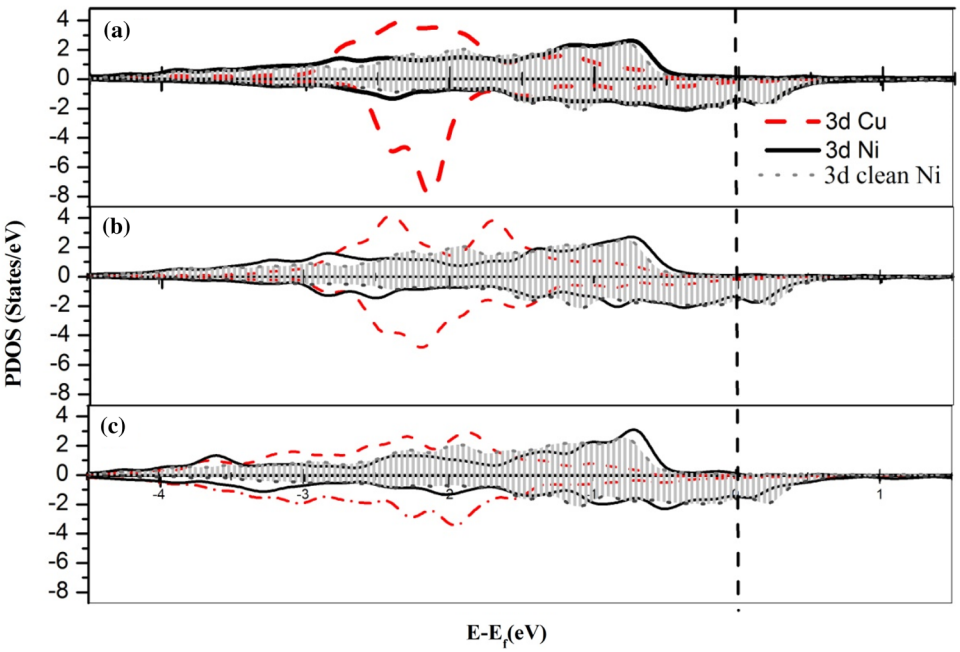

Fig. 4 PDOS of Cu/Ni(100)-(2 × 2) system with different coverages **a** 0.25 ML, **b** 0.50 ML, **c** 1.00 ML. Black solid line for 3*d* Ni topmost atom, red dash line for 3*d* Cu and the dot shaded light grey for 3*d* Ni topmost atom in clean Ni(100) surface (for interpretation of the references to color in this figure legend, the reader is referred to the web version of the article)

the adsorption of Co on Ni(100) surface enhances the magnetic moments of Ni as well as Co compared with their values at bulk and clean surface [29]. Karpuz et al. reported that the increase of Co contents in Co–Ni films increases the saturation magnetization (M_s) since M_s for the bulk Co is higher than that for bulk Ni [30].

The adsorption of ferromagnetic atoms Fe and Co enhances the magnetic moment of Ni topmost surface layer. In addition, Fe and Co maintain their ferromagnetic properties, because their 3*d* wave functions are well localized and the majority bands are filled.

3.3 Cu/Ni(100) system

The structural properties of Cu/Ni(100) system is shown in Table 1. Cu–Ni bonds are the largest bonds for all coverages comparing with Fe–Ni and Co–Ni bonds which predicts the less stability of Cu on Ni(100) surface. Similar to Fe and Co, Cu/Ni(100) system has a pseudomorphic growth at 1.00 ML coverage since Cu–Cu bond is equal to Ni–Ni bond (2.51 Å). The change in the interlayer distances related to their values in the clean Ni(100) surface are very weak at all coverages which reflects the small interaction between 3*d* bands of Ni and Cu due to the fully occupied majority and minority states at Cu. The Cu–Ni bond change slightly as the coverage increase due to the small misfit (f) between Ni and Cu lattice constants $f = (a_{Cu} - a_{Ni})/a_{Cu} = 2.5\%$ and both of them have the cubic fcc crystal structure. Liu et al. found similar misfit (2.5%) for Cu/Ni(100) system [31].

The PDOS of 3*d* bands for Cu/Ni(100) system at 0.25, 0.50 and 1.00 ML coverage are shown in Fig. 4. The *d* band width in Cu/Ni(100) system is smaller than that for Fe/Ni(100) and Co/Ni(100) systems.

Table 3 Magnetic moments for each layers in M/Ni(100) systems in μ_B

System	M (S + 1)	S (Ni surface)	S-1	S-2	S-3
Clean		0.75	0.69	0.69	0.65
Fe					
Θ = 0.25	3.27	0.73	0.64	0.67	0.66
Θ = 0.50	3.30	0.78	0.60	0.66	0.67
Θ = 1.00	2.94	0.69	0.64	0.67	0.68
Co					
Θ = 0.25	2.07	0.75	0.65	0.67	0.66
Θ = 0.50	2.05	0.78	0.62	0.66	0.67
Θ = 1.00	1.89	0.72	0.64	0.68	0.69
Cu					
Θ = 0.25	0.02	0.68	0.69	0.69	0.67
Θ = 0.50	0.02	0.60	0.67	0.67	0.65
Θ = 1.00	0.01	0.52	0.69	0.70	0.69

The *d* band center for the minority spin of Ni at Cu/Ni(100) system change slightly and more than the *d* band center of the Ni majority as can be seen from Table 2 due to the weakly hybridization between the fully occupied *d* bands in Cu and Ni *d* band. The *d* band center of the majority (minority) spin for the topmost Ni surface atom at this system shifts to the left compared with the *d* band center of the topmost Ni atom at Ni(100) clean surface by 0.01(0.09), 0.03 (0.17) and 0.05 (0.26) eV, for 0.25, 0.50 and 1.00 ML, respectively.

The *d* band center for the majority (minority) Cu at 0.50 ML coverage shifts slightly to the right by 0.05 (0.04) eV compared with its value at 0.25 ML coverage. Also, the *d* band center for the majority (minority) Cu at 1.00 ML coverage shifts slightly to the left by 0.31 (0.34) eV compared with its value at 0.25 ML coverage.

The magnetic moment of Ni decreases as the coverage of Cu increases due to the increase in Cu–Cu a well as Cu–Ni hybridization, as can be seen in Fig. 4. This behavior is similar for Ni monolayer over Cu(001) substrate where the magnetic moment of Ni is found to be lower than that of bulk Ni [32]. Karis et al. investigated the properties of Cu/Ni(100) thin films with 1–4 ML coverages by using x-ray absorption spectroscopy in combination with DFT. Their results indicate strong hybridization between the minority spin states at Cu/Ni interface boundary which is consistent with our results [33].

The adsorption of Cu on Ni(100) surface has a slightly effect on Cu magnetic properties due to the interaction between 3*d* bands, which increase the hybridization and decrease the magnetic moment of Ni compared with its value in the clean surface [34]. Ernst et al. concluded from analyzing the density of states of Ni/Cu systems that the hybridization between Ni–Ni and the Ni-Cu has mainly effect on the magnetic properties of Ni and Cu [32].

Our calculations reveal that there is no clear relationship between the *d* band-center and the magnetic moments of the Ni surface layer which are consistent with previous studies [11, 12, 35, 36].

4 Conclusions

In this study structural, electronic, and magnetic properties of M/Ni(100); M = Fe, Co, and Cu systems are investigated at 0.25, 0.50 and 1.00 ML coverage. The calculations are based on DFT in the GGA functional. Ferromagnetic configuration is found to be more stable than non-magnetic configuration for all studied elements. The magnetic moment of Fe and Co are enhanced when they adsorbed on Ni(100) surface at all coverage. Whereas, Cu decreases the FM properties of the topmost Ni(100) surface atom and kept almost non-magnetic.The obtained

results are explained by Hammer- Nørskov model to predict the change on the reactivity of Ni surface by adding the adsorbed metals. The calculations reveal that there is no clear relationship between the *d* band-center and the magnetic moments of the Ni surface layer.

Compliance with ethical standards

Conflict of interest On behalf of all authors, the corresponding author states that there is no conflict of interest.

References

1. Tomishige K (2007) Oxidative steam reforming of methane over Ni catalysts modified with noble metals. Jpn Petrol Inst 50:287–298. https://doi.org/10.1627/jpi.50.287
2. Aspera SM, Arevalo RL, Shimizu K, Kishida R, Kojima K, Linh NH, Nakanishi H, Kasai H (2017) First principle calculations of transition metal binary alloys: phase stability and surface effects. J Elect Materi 46:3776–3783. https://doi.org/10.1007/s11664-017-5402-3
3. Mohsenzadeh A, Bolton K, Richards T (2015) Oxidation and dissociation of formyl on Ni(111), Ni(110) and Ni(100) surfaces: a comparative density functional theory study. Top Catal 58:1136–1149. https://doi.org/10.1007/s11244-015-0482-x
4. Chen Y, Kolhatkar AG, Zenasni O, Xu Sh, Lee TR (2017) Biosensing using magnetic particle detection techniques. Sensors 17:2300. https://doi.org/10.3390/s17102300
5. Kassab S, Erikat I, Hamad B, Khalifeh J (2019) First principles calculations of the energetic, structural, electronic, and magnetic properties of Fe/Ir(100) system. J Elect Materi 48:6932–6939. https://doi.org/10.1007/s11664-019-07509-8
6. Wu H, Parola V, Pantaleo G, Puleo F, Venezia AM, Liotta LF (2013) Ni-based catalysts for low temperature methane steam reforming: recent results on Ni-Au and comparison with other Bi-Metallic systems. Catal 3:563–583. https://doi.org/10.3390/catal3020563
7. Liu CJ, Ye JY, Jiang JJ, Pan YX (2011) Progresses in the preparation of coke resistant Ni-based catalyst for steam and CO_2 reforming of methane. ChemCatChem 3:529–541. https://doi.org/10.1002/cctc.201000358
8. Myint M, Yan Y, Chen JG (2014) Reaction pathways of propanal and 1-propanol on Fe/Ni(111) and Cu/Ni(111) bimetallic surfaces. J Phys Chem C 118:11340–11349. https://doi.org/10.1021/jp501208q
9. Alonso DM, Wettstein SG, Dumesic JA (2012) Bimetallic catalysts for upgrading of biomass to fuels and chemicals. Chem Soc Rev 41:8075–8098. https://doi.org/10.1039/c2s35188a
10. Ch Enger B, Holmen A (2012) Nickel and fischer-tropsch synthesis. Catal Rev Sci Eng 54:437–488. https://doi.org/10.1080/01614940.2012.670088
11. Theofanidis SA, Galvita VV, Poan H, Marin GB (2015) Enhanced carbon-resistant dry reforming Fe–Ni catalyst: role of Fe. ACS Catal 5:3028–3039. https://doi.org/10.1021/acscatal.5b00357
12. Luches P, Gazzadi GC, di Bona A, Marassi L, Pasquali L, Valeri S, Nannarone S (1999) Epitaxial growth of ultrathin Fe films on Ni(001): a structural study. Sur Sci 419:207–215. https://doi.org/10.1016/S0039-6028(98)00792-4
13. O'Brien WL, Tonner BP (1995) Room-temperature magnetic phases of Fe on fcc Co(001) and Ni(001). Phys Rev B 52:15332–15340. https://doi.org/10.1103/physrevb.52.15332
14. Sljivancanin ZV, Vukajlovic FR (1998) Magnetic moments of transition metals overlayers on fcc Ni surface. J Phys: Condens Matter 10:8679–8686. https://doi.org/10.1088/0953-8984/10/39/007
15. Niklasson AMN, Johansson B, Skriver HL (1999) Interface magnetism of 3d transition metals. Phys Rev B 91:6373–6382. https://doi.org/10.1103/PhysRevB.59.6373
16. Gonzalez-delaCruz VM, Pereñiguez R, Ternero F, Holgado JP, Caballero A (2012) In situ XAS study of synergic effects on Ni–Co/ZrO2 methane reforming catalysts. J Phys Chem C 116:2919–2926. https://doi.org/10.1021/jp2092048
17. Zhang J, Wang H, Dalai AK (2007) Development of stable bimetallic catalysts for carbon dioxide reforming of methane. J Catal 249:300–310. https://doi.org/10.1016/j.jcat.2007.05.004
18. Wang Sh, Liao X, Cao D, Huo Ch, Li Y, Wang J, Jiao H (2007) Factors controlling the interaction of CO_2 with transition metal surfaces. J Phys Chem C 111:16934–16940. https://doi.org/10.1021/jp074570y
19. Nørskov JK, Bligaard T, Rossmeisl J, Christensen CH (2009) Towards the computational design of solid catalysts. Nat Chem 1:37–46. https://doi.org/10.1038/nchem.121
20. Giannozzi P, Baroni S, Bonini N, Calandra M, Car R, Cavazzoni C, Ceresoli D, Chiarotti GL, Cococcioni M, Dabo I, Dal Corso A, de Gironcoli S, Fabris S, Fratesi G, Gebauer R, Gertsmann U, Gougoussis C, Kokalj A, Lazzeri M, Martin- Samos L, Marzari N, Mauri F, Mazzarello R, Paolini S, Pasquarello A, Paulatto L, Sbraccia C, Scandolo S, Sclauzero G, Seitsonen AP, Smogunov A, Umari P, Wentzcovitch RM (2009) Quantum Espresso: a modular and open-source software project for quantum simulations of materials. J Phys: Condens Matter 21:395502. https://doi.org/10.1088/0953-8984/21/39/395502
21. Perdew JP, Burke K, Ernzerhof M (1996) Generalized gradient approximation made simple. Phys Rev Lett 77:3865–3868. https://doi.org/10.1103/PhysRevLett.77.3865
22. Kittel C (1986) Introduction to solid state physics, 6th edn. Wiley, New York
23. Danan H, Herr A, Meyer A (1968) New determinations of the saturation magnetization of nickel and iron. J Appl Phys 39:669–670. https://doi.org/10.1063/1.2163571
24. Monkhorst HJ, Pack JD (1976) Special points for Brillouin-zone integrations. Phys Rev B 13:5188–5192. https://doi.org/10.1103/PhysRevB.13.5188
25. Methfessel M, Paxton AT (1989) High-precision sampling for Brillouin-zone integration in metals. Phys Rev B 40:3616–3621. https://doi.org/10.1103/PhysRevB.40.3616
26. Rodriguez JA, Goodman DW (1992) The nature of the metal-metal bond in bimetallic. Surf Sci 257:897–903. https://doi.org/10.1126/science.257.5072.897
27. Hammer B, Nørskov JK (1995) Electronic factors determining the reactivity of metal surfaces. Surf Sci 343:211–220. https://doi.org/10.1016/0039-6028(96)80007-0
28. Mizutani U (2003) Introduction to the electron theory of Metals. Cambridge University Press, Cambridge, p 400
29. Niklasson AMN, Johansson B, Skriver HL (1999) Interface magnetism of 3d transition metals. Phys Rev B 59:6373–6382. https://doi.org/10.1103/PhysRevB.59.6373
30. Karpuz A, Kockar H, Alper M (2013) Electrodeposited Co–Ni films: electrolyte pH—property relationships. J Supercond Nov Magn 26:651–655. https://doi.org/10.1007/s10948-012-1774-z
31. Liu K, Zhang RF, Beyerlein IJ, Chen XY, Yang H, Germann TC (2016) Cooperative dissociations of misfit dislocations at bimetal interfaces. APL Materials 4:111101. https://doi.org/10.1063/1.4967207
32. Ernst A, Lueders M, Temmerman WM, Szotek Z, van der Laan G (2000) Theoretical study of magnetic layers of nickel on copper; dead or alive? J Phys Condens Matter 12:5599–5605. https://doi.org/10.1088/0953-8984/12/26/306

33. Karis O, Magnuson M, Wiell T, Weinelt M, Wassdahl N, Nilsson A, Mårtensson N, Holmström E, Niklasson AMN, Eriksson O (2000) Observation of short- and long-range hybridization of a buried Cu monolayer in Ni. Phys Rev B 62:R16239–16242. https://doi.org/10.1103/PhysRevB.62.R16239
34. Blügel S S (2005) Reduced dimensions: Magnetic moment and magnetic structure. In: Magnetism goes Nano, volume 36 of Spring School lecture notes of Institute of Solid state Research. Schriften des Forschungszentrums Julich, pp 10–25
35. Hofmann T, Yu TH, Folse M, Weinhardt L, Bär M, Zhang Y, Merinov BV, Myers DJ, Goddard WA, Heske C (2012) Using photoelectron spectroscopy and quantum mechanics to determine d–band energies of metals for catalytic applications. J Phys Chem C 116:24016–24026. https://doi.org/10.1021/jp303276z
36. Nonas B, Wildberger K, Zeller R, Dederichs P (1997) Ab-initio calculations for 3d impurities on Fe(001) and Ni(001). J Magn Magnet Mater 165:137–140. https://doi.org/10.1016/S0304-8853(96)00489-1